PERIODICO di MINERALOGIA
established in 1930

An International Journal of
MINERALOGY, CRYSTALLOGRAPHY, GEOCHEMISTRY, ORE DEPOSITS, PETROLOGY, VOLCANOLOGY
and applied topics on *Environment*, *Archaeometry* and *Cultural Heritage*

Characterization and origin of alunite in the El-Gideda iron mine (Egypt)

MERVAT HASSAN* and HASSAN BAIOUMY

Central Metallurgical R & D Institute, P.O. Box 87, Helwan, Cairo, Egypt

Submitted, October 2006 - Accepted, December 2006

ABSTRACT. — Alunite in El-Gideda iron mine, Bahria Oasis, occurs as very soft and light white to pinkish beds and pockets ranging in thickness from few cm to 0.5 m intercalated with glauconites of the Hamra Formation. The fine scale mineralogy was determined using XRD, SEM, DTA, TG, IR and XRF. Alunite is the main constituent, and jarosite was detected as a minor mineral. Hydrated halloysite is the main aluminum silicate mineral associated with alunite in varying proportions. Gibbsite and trace of quartz are also detected. Iron oxides are represented by iron-oxyhydroxide (goethite) in size and shape similar to that of bacterial iron mineralization. Amorphous silica was recorded in SEM image and IR spectra. Morphology of alunite ranged from tubular or flatten rhombohedral to well crystallized cubes. This is very characteristic for supergene alunite formed by oxidation of sulfides in a K-rich environment. Due to acid alteration of sulfate, glauconites of the overlying Hamra Formation were altered and released K, Al, Si, and Fe. The former three elements form alunite and halloysite. Iron forms at least a part of the iron ore in the El-Gideda mine. Glauconite intercalated by alunite is highly destabilized with fractured pellets and iron rims as well as low potassium content. Therefore, alunite and halloysite can be considered as by-products of weathering of the intercalated glauconites in an environment of sulfide oxidation (i.e., high Eh, low pH together with biological activities).

* Corresponding author, E-mail: mervathassan@hotmail.com

RIASSUNTO. — L'alunite della miniera di ferro di El-Gideda, nell'Oasi di Bahria, si rinviene in letti poco coerenti di colorazione variabile dal bianco chiaro al rosato o in tasche di spessore compreso tra pochi centimetri e mezzo metro; il minerale è intercalato alla glauconite della Formazione di Hamra. Le analisi di dettaglio riguardanti la mineralogia sono state eseguite tramite XRD, SEM, DTA, TG, IR e XRF. Assieme all'alunite, minerale predominante, è stata identificata la presenza di jarosite. L'halloysite idrata è il principale silicato di alluminio associato all'alunite in varie proporzioni; sono stati anche riscontrati gibbsite e tracce di quarzo. Gli ossidi di ferro sono rappresentati da goethite con dimensioni e forme analoghe a quelle delle mineralizzazioni di ferro di origine batterica. Silice amorfa è stata rilevata tramite immagini SEM e spettri IR. La morfologia dell'alunite varia da romboedri tubolari o appiattiti a forme cubiche ben cristallizzate. Tali caratteri sembrano tipici di aluniti supergeniche formate per ossidazione di solfuri in ambienti ricchi di K. A seguito della trasformazione dei solfati in ambiente acido, le sovrastanti glauconiti della Formazione

di Hamra hanno subito alterazioni con rilascio di K, Al, Si, e Fe. I primi tre elementi hanno formato l'alunite e l'halloysite mentre il ferro ha contribuito alla formazione di almeno una parte degli adunamenti della miniera di El-Gideda. La glauconite intercalata all'alunite è in fase di avanzata destabilizzazione essendo costituita da porzioni tipo pellets fratturati con bordi costituiti da ferro ed anche da discrete quantità di potassio. Pertanto, l'alunite e l'halloysite possono essere considerate quali prodotti di trasformazione in ambiente meteorico delle originarie glauconiti intercalate in ambienti di ossidazione di solfuri ossia con alto Eh, basso pH, unitamente ad attività di tipo biologico.

KEY WORDS: *Bahria Oasis, Egypt, gibbsite, alunite, glauconites, jarosite, weathering.*

INTRODUCTION

Alunite is one of the minerals of the alunite supergroup (see Jambor 1999, Canadian Mineralogist for recent classification). Its ideal chemical formula is $KAl_3(SO_4)2(OH)$ and it generally has rhombohedral or hexagonal habit. It is colourless in the pure state, but is found in grey-white, yellow-white and reddish colours due to impurities in its structure. The alunite is formed during alteration of aluminum- and potassium-bearing materials such as clay minerals and K-feldspars in acid-sulfate environment; i.e., high Eh, low pH (Kelepertsis, 1989; Long, *et al.*, 1992; Rye, *et al.*, 1992; Mutlu, *et al.*, 2005). Similarly, alunite is formed during H_2SO_4 speleogenesis of the Guadalupe caves, sulfuric acid interaction with clays that contain potassium such as illite and montmorillonite (Polyak and Güven, 1996; Polyak and Provencio, 1998; Polyak and Güven, 2000; Polyak and Provencio, 2001). We report an alunite occurrence in the El-Gideda iron mine, Bahria Oasis, as very soft, light and whiteto pinkish beds and pockets ranging from few cm to 0.5 m in thickness intercalated with glauconites of the Hamra Formation. Detailed mineralogical and geochemical studies of glauconites of the Hamra Formation (El–Sharkawi and Kalil, 1977; Masaed and Surour, 1999; Dabous, 2002; Hassan and Baioumy, 2003; Hassan and El-Shall, 2004; Bioumy and Hassan, 2004) revealed intensive weathering of glauconite under humid-wet conditions prevailed in the Bahria Oasis during the late Eocene. According to these authors, glauconites of the Hamra Formation show different stages of alteration. In the slightly altered zones, the glauconitic matrix is first destabilized with the progressive leaching of interlayer cations (mainly K), and tetrahedral Si of the dioctahedral structure. Towards the upper part of this horizon, the matrix becomes highly disturbed and consists entirely of amorphous argillaceous material of mixed layers of Fe-bearing smectite and kaolinite with micron-sized iron hydroxide particles. The glauconite pellets are progressively fractured, and their Fe in them is redistributed as dark amorphous iron hydroxide.

The aim of this study is to describe the mineralogy, geochemistry and the origin of these alunite lenses and layers found within the glauconitic clay of the El-Gideda iron mine.

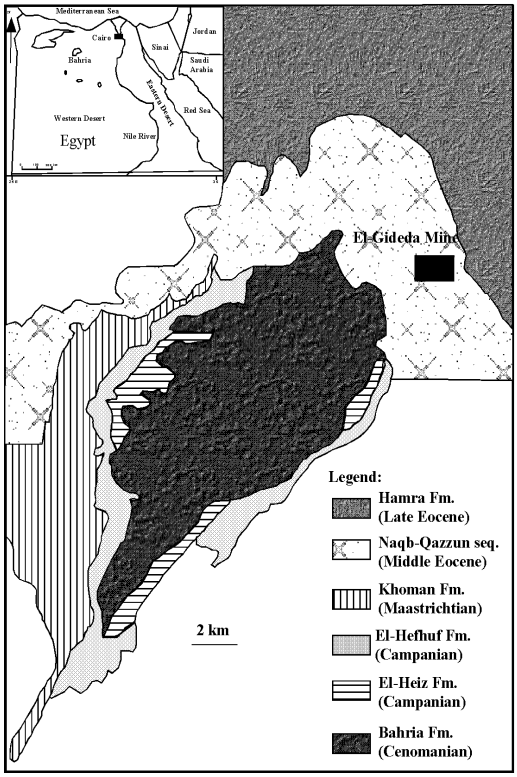

Fig. 1 – Geological map showing the location of the studied area.

Geological Setting and Stratigraphy

The Bahria Oasis is a large depression in the Western Desert of Egypt with hot, dry climatic conditions. It is located about 270 km SW of Cairo and 180 km west of the Nile Valley (Fig. 1), and is of special interest due to the presence of great reserves (270 million metric tones) of iron ore deposit (Said, 1990).

The El-Gideda mine area (Fig. 1) is an oval shaped depression up to 15 km^2, situated within the degraded karst cone hills of the Naqb Formation of Middle Eocene age. The central part of the depression is characterized by a high relief (up to 254 m above sea level). The low Wadi area, up to 198 m a.s.l., surrounds the high central area, which is built up by the Cenomanian clastics at the base, overstepped by the main Lutetian iron ore successions. In the Eastern and Western Wadi areas, the ore successions are truncated unconformably by late Lutetian-Bartonian glauconitic sediments with lateritic ironstone interbeds of the Hamra Formation (Fig. 2). The iron ore and the overlying glauconitic sediments are folded and undulated. The iron ore sequence attains its maximum thickness, up to 35 m, in the Western and Eastern Wadi areas, reduced into 11 m in the high central area. This iron ore sequence consists of a pisolitic-oolitic iron stone unit followed by highly karstified-bedded ferruginous dolostones and mudstones. Ore conglomerates mixed with silicified limestone and chert overly the karst ore. The genesis of the ores has been a matter of a scientific discussion for a long time. El-Sharkawi and Khalil (1977) distinguished three genetic types of the El-Gideda iron ore: (1) massive hydrothermal metasomatic; (2) porous or massive, derived from mobilized iron and manganese redeposit in fresh water lakes, possibly through biogenic activity; (3) a product of the weathering of glauconitic clays and sands, usually with an oolitic or pisolitic texture. Dabous (2002) supported the hypothesis that the ore is epigenetic of fresh groundwater origin and formed in two different stages: (1) the iron is oxidized and leached from the sandstone of the Nubia Aquifer by upward-moving of hot groundwater and deposited in the overlying pre-existing Lower-Middle Eocene Karstic limestone, in the first stage under a dry climatic condition; (2) the iron is then leached from the glauconitic clayey beds, infiltrated downwards and deposited on the underlying primary ore in the successive wet pluvial periods. During these two stages, initial structures, variation in pH-Eh, and biological activities were the main factors controlling the deposition and character of the ore.

The thickness of the overlying glauconitic sediments varies from up to 25 m in the Western and Eastern Wadi areas to less than 1 m in the high central area. According to Mesaed and Surour (1999), the glauconite facies of the El-Gideda mine area represents deposition in a shallowing-upward regime and consists of two large-scale cycles: 1) stratiform syndiagenetic glauconitic ironstone pockets and concretions predominating within the lower parts of the small-scale cycles; 2) lateritic glauconitic ironstones, which formed during intermittent periods of subaerial weathering and lateritization of the parental glaucony facies.

Methodology

Samples representing the pure alunite horizons (H16, H18, H23, H24, H26 and H28) as well as alunite with gibbsite (Block 9) and alunite with halloysite (W5) were subjected to mineralogical and geochemical analyses. Alunite samples are white to grayish and yellowish white and very soft while samples with gibbsite and halloysite are yellow to gray and relatively harder.

A Philips PW 1730 powder XRD with Ni-filtered Co K_α run at 40 kV and 25 mA was used to examine both the bulk samples and clay fractions. 8 bulk samples were analyzed in the 2°° to 80°° 2θ range and clay fractions in the 2°° to 40° in 2θ range. Powder pellets of representative samples were analyzed for their major oxides (SiO_2, TiO_2, Al_2O_3, Fe_2O_3, MnO, MgO, CaO, K_2O, Na_2O, SO_3, Cl and P_2O_5) by XRF using a Philips PW 2400 X-ray spectrometer at the Geological Survey of Egypt. Tube voltage and current for W target were 40 kV and 60 mA, respectively. L.O.I. was obtained by heating sample powders to 1000°C for 7 h. Morphology and chemistry of alunite and associated minerals were studied with a Philips S-2400s SEM-EDX at the Geological Survey of Egypt. Four 200 mg samples were analyzed with a Netzsch STA 409 simultaneous thermal analysis apparatus between room temperature and 1100°C

at a heating rate of 10°C/min. Alumina was used as a reference material. Infrared vibrational spectra were recorded on a Pye-Unicam SP 300 Fourier transform spectrometer at Cairo University, Egypt.

For each sample, 128 scans were recorded in the spectral range of 4000-400 cm^{-1} within the transmittance mode and a resolution of 4 cm^{-1}. The KBr pressed disks were prepared with 0.4 mg of sample and 200 mg of KBr.

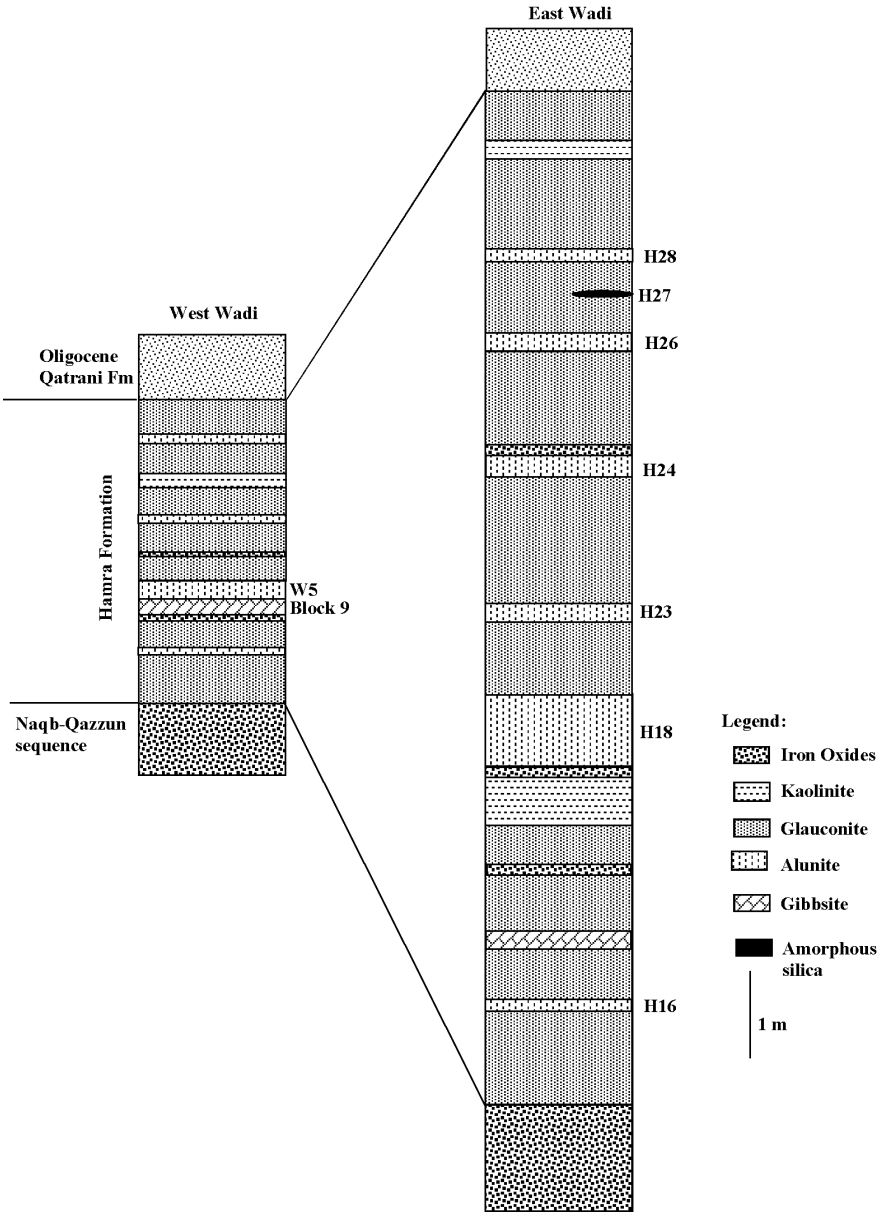

Fig. 2 – Lithostratigraphy of the studied sections showing the locations of the analyzed samples.

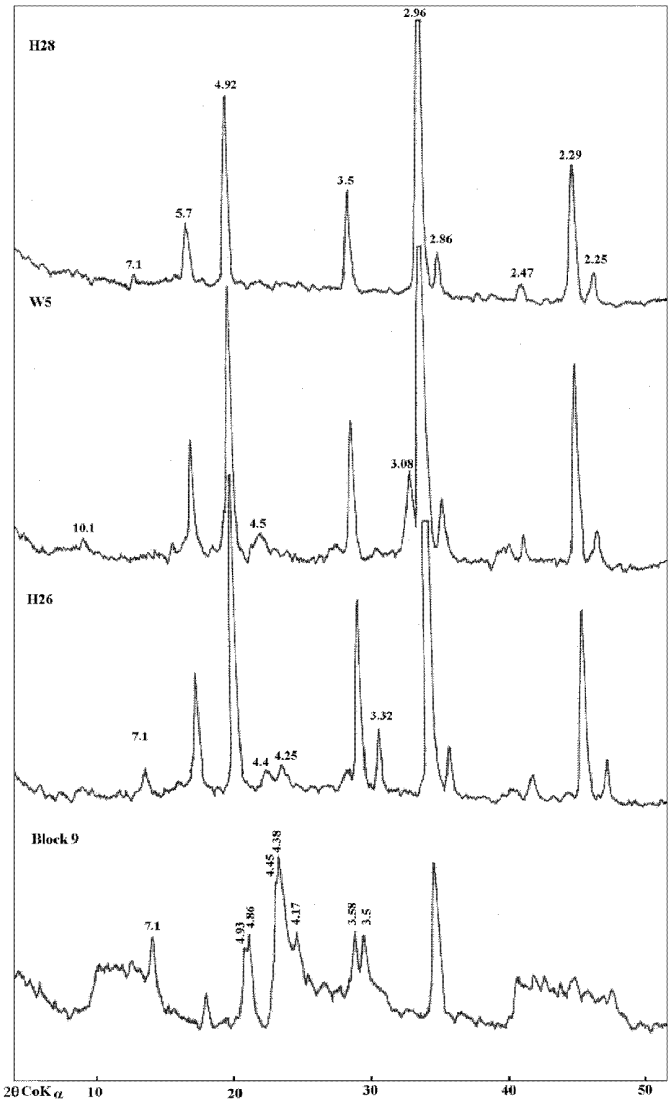

Fig. 3 – XRD patterns of representative samples.

Results

Mineralogy

The XRD patterns (Fig. 3 and Table 1) indicated that, sulfate minerals are abundant in all samples and alunite group minerals are the major constituent. Jarosite was detected only as a minor phase, while little mica (muscovite) is present in sample W5. XRD pattern of halloysite and gibbsite rich sample (Block 9) is characterized by very broad 001 and 002 reflections of halloysite-10Å. The 001 reflection is spread between 10 and 14.2° in 2θ. A diagnostic feature of the XRD pattern of

TABLE 1
Powder X-ray diffraction data of studied samples

Block 9		W5		H16		H18		H23		H24		H26		H28		Min.
d Å	I/I0	d Å	I/I0	d Å	I/I0	d Å	I/I0	d Å	I/I0	d Å	I/I0	d Å	I/I0	d Å	I/I0	
---		10.1	6	---		---		---		---		---		---		Mi
10.1 -7.19	46	---		---		---		---		---		7.19	6	7.19	4	Ha
5.7	23	5.7	22	5.7	26	5.7	23	5.7	17	5.7	27	5.7	22	5.7	15	Al
4.92	53	4.92	49	4.92	56	4.96	53	4.92	41	4.92	67	4.92	56	4.92	43	Al
4.82	60	---		---		---		---		---		---		---		Gi
---		4.5	8	---		---		---		---		---		---		Mi
4.45	91	---		---		---		---		---		4.45	6	---		Ha
4.38	10	---		---		---		---		---		---		---		Gi
---		---		4.24	4	4.25	3	---		---		4.24	7	---		Qz
3.58	61	---		---		---		---		---		3.58	6	--		Ha
4.17	62	---		---		---		---		---		---		---		Go
3.50	62	3.50	26	3.50	32	3.5	33	3.5	25	3.5	38	3.5	33	3.5	22	Al
---		---		3.34	4	3.33	3	---		---		3.34	12	---		Qz
---		3.12	11	---		---		--		---		---		---		Ja
---		3.09	12	---		---		---		---		---		---		Ja
2.96	100	2.96	100	2.96	100	2.96	100	2.96	100	2.96	100	2.96	100	2.96	100	Al
---		2.86	12	2.86	11	2.89	11	2.86	10	2.86	15	2.86	9	2.86	9	Al
---		2.5	7	2.5	2	---		---		2.5	11			---		Al
---		2.47	7	2.48	4	2.49	6	2.48	3	2.48	8	2.48	5	2.48	5	Al
---		2.29	33	2.29	37	2.29	39	2.29	33	2.29	42	2.29	31	2.29	29	Al
---		2.21	7	2.21	9	2.21	9	2.21	6	2.21	12	2.21	8	2.22	8	Al

Mi = Mica; Ha = Halloysite; Al = Alunite; Gi = Gibbsite; Qz = Quartz; Go = Goethite; Ja =Jarosite

halloysite is that the 11, 02 reflections at 4.45Å are more intense than basal reflections. Halloysite-7Å or other kaolin minerals were detected as a minor constituent in samples H18, H26 and H28. The sample Block 9 contains detectable amount of gibbsite, which can be recognized by its characteristic reflection lines at 4.89 and 4.38 Å, associated with trace amount of goethite. Quartz is evidenced in the samples H16, H18, and H26 patterns as a minor constituent. The mineralogy of clay fraction (≤ 2 μm) revealed the presence of highly hydrated halloysite (~10Å) which is characterized by a very broad and diffuse 001 reflection between 10.4 and 13.6° in 2θ (Baioumy and Hassan, 2004).

The DTA and TG curves (Figs. 4 and 5) of alunite–rich samples show two endothermic reactions with rapid losses of weight in the regions 489ºC -624ºC and 733ºC -933ºC followed by gradual loss of weight up to 1000ºC. The first endothermic reaction is due to dehydration and decomposition of alunite to $KAl(SO_4)_2$ and amorphous Al_2O_3 (Küçük and Gülaboğlu, 2002). The second endothermic one is due to decomposition of $KAl(SO_4)_2$ into K_2SO_4 (arcanite) and Al_2O_3 phases (Kakali *et al.*, 2001).

DTA curve of halloysite-gibbsite sample (Block 9) shows a low-temperature endothermic reaction up to 130°C, which may be attributed to loss of absorbed water molecules. The second endothermic reaction at a temperature not higher

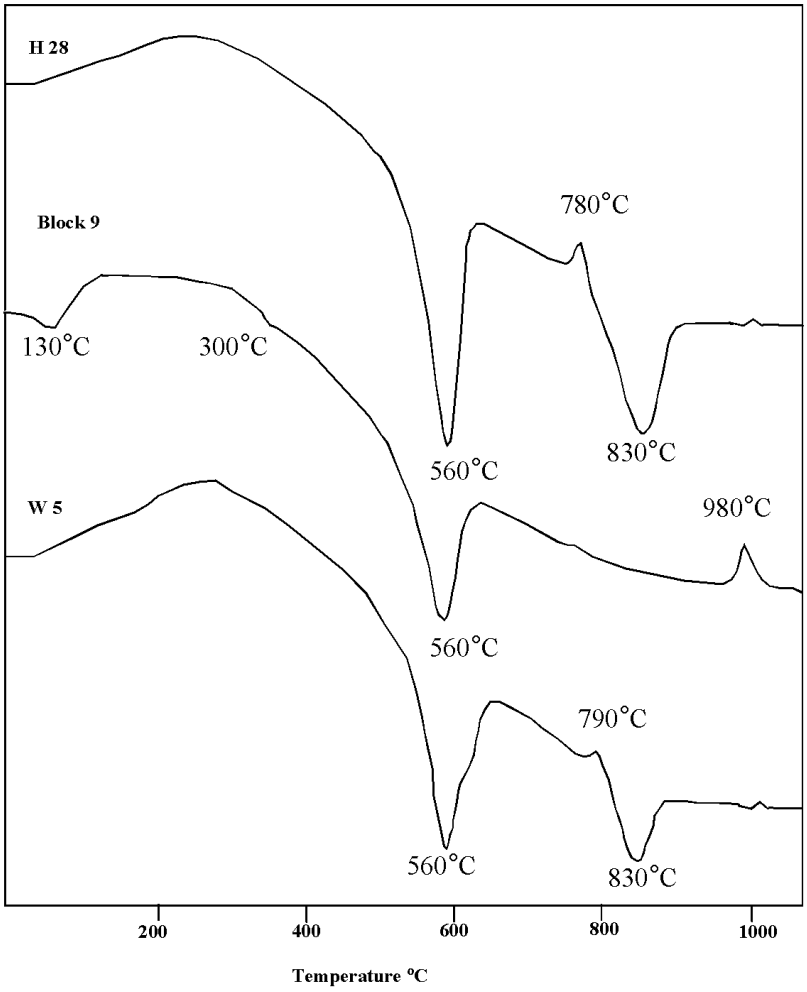

Fig. 4 – DTA curves of representative samples.

than 300ºC corresponds to the dehydroxylation of gibbsite and goethite that could also be identified in the XRD pattern of Block 9. Dehydroxylation of halloysite was observed at around 560°C. Depending on crystallinity and other factors, kaolinite decomposition temperatures are variable in an ample range. High-temperature exothermic reaction at around 980ºC, which was observed for sample Block 9 (Fig. 4), may be reflected to the 'spinel-transition', a change in the packing of oxygen ions of the metakaolinite structure leading to regions of an Al-Si spinel together with disordered Si-rich region. Mullite forms from these materials at a higher temperature (Kakali *et al.*, 2001). The intensity of this exothermic peak increases depending on the halloysite content.

The amounts of different types of water (free water and crystallization water) in Block 9, as well as evolution of sulfur compounds, were estimated G the TG curves (Fig. 5). The weight loss due to dehydration of hydrated halloysite (as a result of dehydroxylation of gibbsite and goethite) and

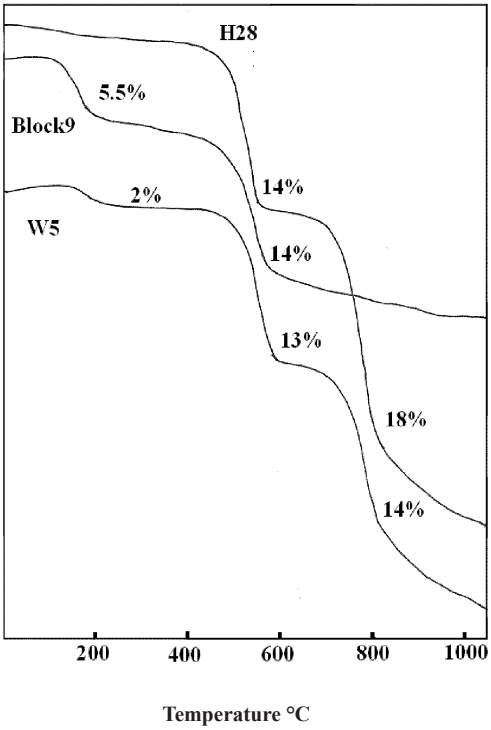

Fig. 5 – TG curves of representative samples.

weight loss due to the dehydroxylation of halloysite and desulphurization of alunite correspond to 5.5% and 14%, respectively.

IR spectra of the alunite-rich sample (H28 in Fig. 6) are characterized by absorption bands at 3485, 683, 627, 596 and 527 cm^{-1}. The intensities of these bands decrease with the decrease of alunite contents in the order H28, W5 and Block 9. The IR spectrum of halloysite-gibbsite rich sample (Block 9 in Fig. 6) shows a significant broadening in the OH-stretching site between 3700-3620 cm^{-1} because of structure distortion caused by variable hydration. Russell and Fraser (1995) concluded that the reduction in size of the 3670 cm^{-1} band and broadening of the 3650 cm^{-1} band are typical for the disordered kaolinite. An IR disordered index, defined as I(3670 cm^{-1})/I(3650 cm^{-1}), helps to identify disordering in kaolinite (Muller and Bocquier, 1985).

MORPHOLOGY

The crystal habit of alunite ranges from tubular or flatten rhombohedral (Fig. 7) to well crystalline cubic (Fig. 8). The ''rhombohedra'' are actually a combination of two trigonal pyramids. This morphology is characteristic of supergene alunite formed by the oxidation of sulfides in a K-rich environment (Dabous, 2002). Filamentous algae were recognized by SEM (Fig. 9), fine fibers of hallyosite were adhering to the surface of biomate. These biomate embedded in spherical aggregates of halloysite fibers have a diameter less than 2 μm sometimes <0.1 μm. Gibbsite occurs as euhedral crystals in association with the halloysite fibers (Fig. 10). Spherical or elliptical amorphous materials were recognized in sample H27 (Fig. 11). The size of these materials is almost the same as that of the radial crystal growth recognized in halloysite. Jarosite was found as well-developed crystal aggregates in sample H28 (Fig. 12). This mineral might be the indicator of strongly acidic and oxidizing conditions (Brown, 1971). According to Dabous (2002), jarosite might be the product of transformation of S-bearing Fe precipitates to goethite. Goethite in the form of micrometer-sized chestnut-burr like shapes was recognized in the SEM image of sample Block 9 (Fig. 13). These aggregates are similar in size and shape to bacterial iron mineralization. Kaolinite in booklets and rosette–like shapes (Fig. 12) was found in the sulfate layers in glauconites of the El-Gideda iron mine. According to Nagasawa (1978), kaolinite, halloysite and euhedral crystals of gibbsite are important products of weathering with predominance of aluminum silicate minerals. In deeper portions of the weathering zone (e.g. W5), halloysite is a dominant product of weathering induced by the percolating water. Semi-quantitative EDX analyses of alunite yield strong peaks of S, Al and K as well as trace of Si, while EDX of gibbsite-rich sample (Block 9) revealed strong peaks of Al and Si with traces of K and S (Figs 7 and 8). Amorphous silica sample yielded strong peak of Si with traces of Al, Si and K (Fig. 11).

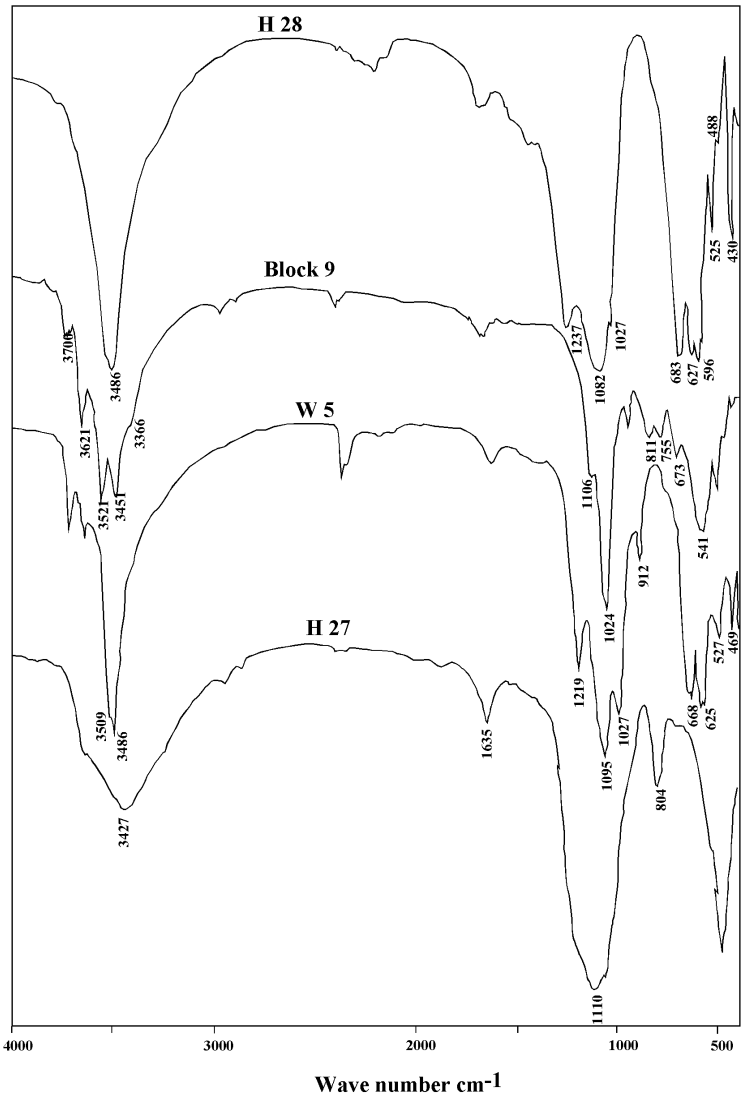

Fig. 6 – IR of representative samples

Chemical Composition

The results of the chemical analysis of 8 samples from the Western and Eastern Wadi sections representing the gibbsite-, halloysite- and alunite-rich rocks are shown in Table 2. Gibbsite- and halloysite-rich samples show high SiO_2 and Al_2O_3 contents whilst alunite-rich samples are characterized by higher Al_2O_3, SO_3 and K_2O contents with a very strong positive correlation between SO_3 and K_2O contents indicating a common source for these two elements (mainly as alunite). From the low Na_2O content, alunite should be dominantly potassic. Iron contents are high in the majority of samples. Other constituents such as TiO_2, MnO_2, CaO, MgO, and Na_2O show low and variable concentrations.

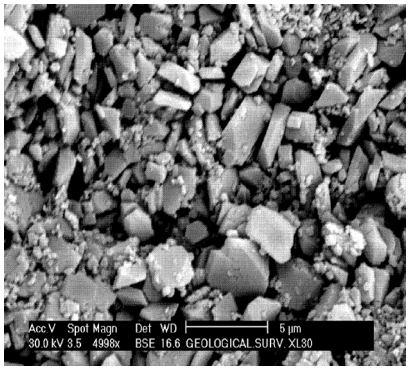

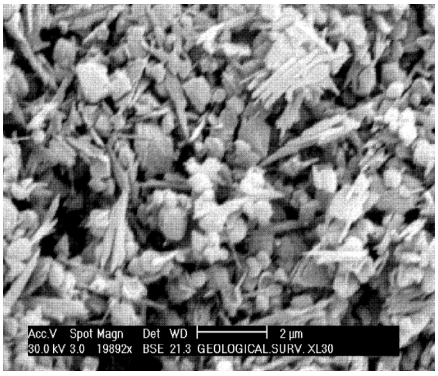

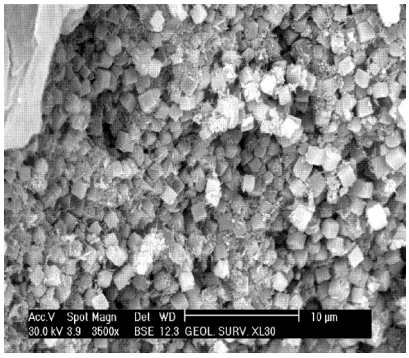

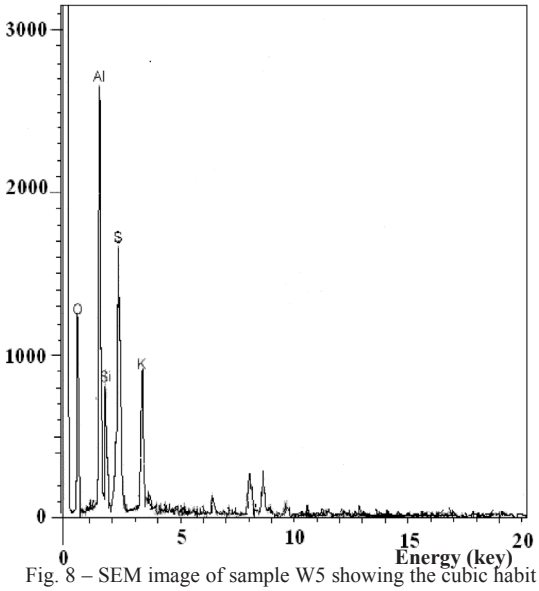

Fig. 8 – SEM image of sample W5 showing the cubic habit of the alunite coated with very fine halloysite fibers with an EDX spectrum.

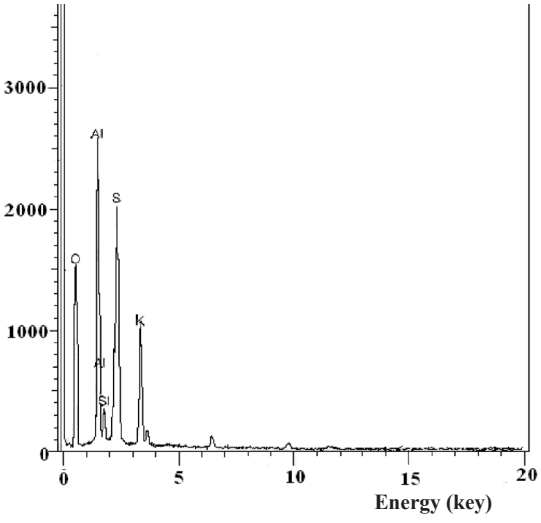

Figure 7: SEM image of sample H18 showing the rhombohedral and cubic habit of the alunite and an EDX spectrum

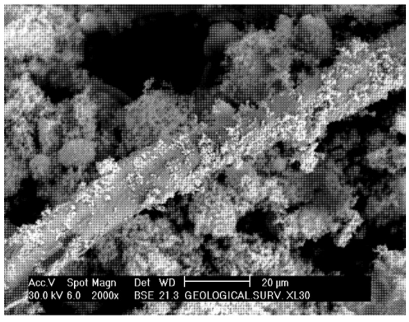

Fig. 9 – SEM of image of sample Block 9 showing the filamentous algae.

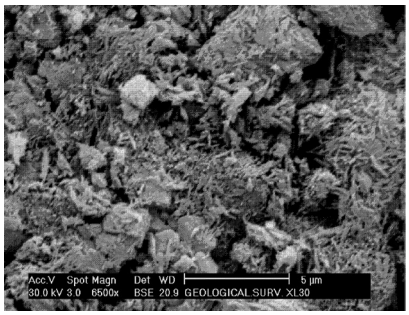

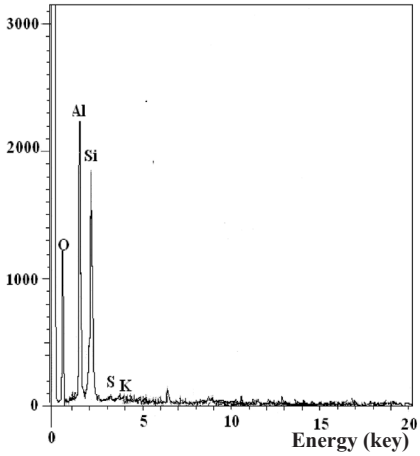

Fig. 10 – SEM of image of sample Block 9 showing the gibbsite crystals (G) within halloysite fibers (H) and an EDX spectrum.

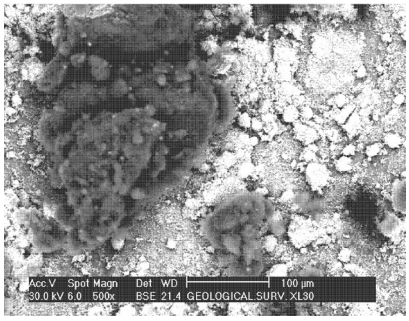

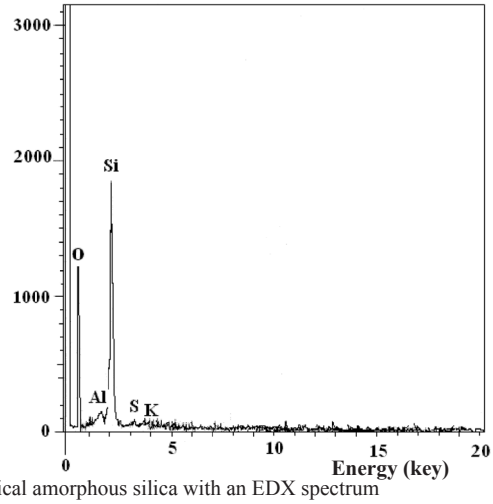

Fig. 11 – SEM image of sample H23 showing spherical and ellipitical amorphous silica with an EDX spectrum

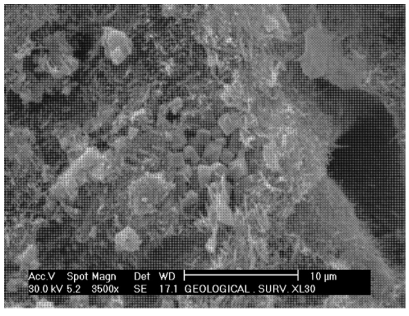

Fig. 12 – SEM image showing well-developed crystals of jarosite (J) coated by fibrous halloysite (H). Booklets and rosette–like kaolinite crystals (K) are also observed.

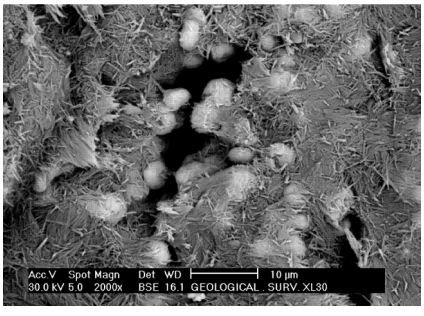

Fig. 13 – SEM image of sample Block 9 showing the micrometer-sized chestnut-burr like goethite within the fibrous halloysite.

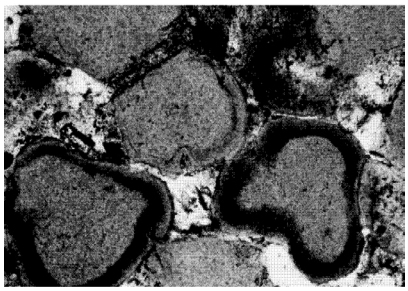

Fig. 14 – Photomicrograph of host glauconites showing the fractures and altered rims.

DISCUSSION

From the previous data it is clear that the thin layers and lenses of alunite intercalated with green to greenish glauconitic materials of the Hamra Formation consists essentially of alunite and trace amount of jarosite, with varying proportions of authigenic minerals such as halloysite, kaolinite, and traces of gibbsite, quartz and amorphous materials. We suggest that the recorded mineral assemblages in the studied area were formed as a result of alteration of the intercalated glauconites of the Hamra Formation. According to El-Sharkawi and Khalil (1977), intense weathering of glauconite in an acid oxidizing environment produced alunite and the releases of silica, alumina and iron, which either were deposited in situ or migrated downwards or replaced the underlying middle Eocene carbonates. In their detailed mineralogical and geochemical studies on the Hamra Formation glauconites, Mesaed and Surour (1999) described different alteration stages changing from slight argillization to lateralization. In the slightly altered zones, the glauconitic matrix is destabilized throughout the progressive leaching of interlayer cations (mainly K) and tetrahedral Si of the dioctahedral structure. Towards the upper part of this horizon, the matrix becomes highly disturbed and consists entirely of amorphous argillaceous material and mixed–layers of Fe-smectite-kaolinite with micron-sized iron hydroxide particles. The glauconite pellets are progressively fractured and their Fe is redistributed as dark amorphous iron hydroxide (Fig. 14). According to Hassan and El-Shall (2004), glauconitic material of the El-Gideda iron mine has low K content (~ 6%), which is attributed to either composition of the parental glaucony mineral or destabilization of glauconite.

TABLE 2

Chemical analysis of alunite layers in the Hamra Formation Bahria Oasis

Oxides (Wt.%)	Gibbsite – rich rock	Halloysite – rich rock	Alunite – rich rock					
	Block 9	W5	H16	H18	H23	H24	H26	H28
SiO_2	34.15	11.16	1.29	4.84	1.95	6.37	4.85	3.73
Al_2O_3	34.38	32.96	35.64	33.50	34.36	31.58	32.22	33.26
TiO_2	0.02	0.19	0.05	0.09	0.06	0.14	0.01	0.01
Fe_2O_3	2.17	6.75	1.23	2.94	0.83	2.8	4.10	5.30
MnO	0.01	0.02	0.01	0.01	0.01	0.01	0.01	0.01
MgO	0.38	0.33	0.23	0.29	0.28	0.27	0.24	0.24
CaO	0.36	0.24	0.11	0.31	0.22	0.21	0.26	0.14
Na_2O	0.36	0.12	0.12	0.12	0.12	0.11	0.11	0.10
K_2O	0.71	6.80	9.96	8.30	9.05	8.63	8.53	8.90
P_2O_5	0.68	0.45	0.34	0.36	0.31	0.39	0.39	0.66
SO_3	1.58	27.95	37.12	34.11	37.19	35.46	35.05	36.58
L.O.I	24.27	13.03	13.90	15.13	15.62	14.03	14.23	11.07
Total	99.07	100	100	100	100	100	100	100

Therefore, glauconite releases Fe, K, Si and Al during the weathering process under strongly acidic oxidizing conditions. Iron forms at least part of the iron ore in the El-Gideda mine while Al forms halloysite and kaolinite and K together with S forms the alunite.

Regarding the source of sulfur required for the formation of alunite, different theories have been put forward. El-Sharkawi and Khalil (1977) suggested volcanic gases or sulfur deposits, which are completely dissolved in surface waters, to be the source of sulfur. Al-Boghdady and Abu El-Hassan (1999) stated that hydrothermal solutions associated with the Tertiary volcanism in the Bahria Oasis as another possible source of sulfur. Abdel-Monem *et al*. (2003) described pyrite beds and lenses in the iron ore that are associated with gypsum as an evidence for the alteration of this pyrite. The present study suggests that the alteration of such pyrite beds and lenses under acidic conditions could be the source of sulfur which is necessary for the alunite formation.

Conclusions

Alunite in the Bahria Oasis was formed as a result of glauconites alteration suggesting an intensive chemical alteration under humid and wet conditions prevailed during the late Eocene. Glauconite alteration releases iron, silica, and alumina. Iron forms at least part of the iron ore in El-Gideda mine while alumina forms alunite, gibbsite and halloysite in an acidic environment.

Acknowledgments

Authors are grateful to Dr. Abbas M. Youssef and Mr. M. Mansour of the Egyptian Steel Company for their help during the fieldwork.

REFERENCES

Abdel-Monem A.M., Qorani, E.A. and Youssef A.M. (2003) – *Occurrence and genesis of pyrite in El-Gideda iron ore mine, El Baharia depression, Western Desert, Egypt.* Sedimentology of Egypt, **11**, 227-233.

Al-Boghdady A.A. and Abu-El-Hassan M.M. (1999) – *Nature of occurrence and origin of the barite at E-Gideda iron ore mine, Bahria Oasis, Egypt.* Geochem. Int., **5**, 536-548.

Baioumy, H. M. and Hassan, M. S., (2004) – *Authigenic halloysite from El-Gideda iron ore, Baharia Oasis, Egypt: characterization and origin.* Clay Mineral, **39**, 207-17.

Brown J.B., (1971) – *Jarosite goethite stabilities at 25 °C and 1 atm.* Mineral. Dep., **6**, 245-257.

Dabous A.A. (2002) – *Uranium isotopic evidence for the origin of the Bahariya iron deposits, Egypt.* Ore Geol. Rev., **19**, 165-186.

El-Sharkawi M.A. and Khalil M.A. (1977) – *Glauconite a possible source of iron for El–Gideda iron ore deposits, Bahria Oasis, Egypt.* Egyptian J. Geol., **21**, 109-116.

Hassan M.S. and Baioumy H. M. (2003) – *Modification of some Egyptian glauconites for industrial applications. Mineral exploration and sustainable Development*, Eliopoulos *et al*. (eds) Proceeding of the Seventh Biennial SGA Meeting Athen/ Greece/ 24-28 August, 907-910.

Hassan M.S. and El- Shall H. (2004) – *Glauconitic clay of El-Gidada, Egypt: evaluation and surface modification.* Appl. Clay Sci., **27**, 219-222.

Kakali G., Perraki T., Tsivilis S. and Badoginnis E. (2001) – *Thermal treatment of kaolin: the effect of mineralogy on the pozzolanic activity.* Appl. Clay Sci., **20**, 73-80.

Kelepertsis A.E. (1989) – *Formation of sulfate at the Thiaphes area of Milos, Island: possible precursors of kaolinite mineralization.* Science, **270**, 1874-1875.

Küçük A. and Gülaboğlu S. (2002) – *Thermal deposition of Şaphane alunite ore.* Industrial Engin. Chimerical Res., **41**, 6028-6032.

Long D.T., Fegan N.E., Mckee J.D., Lyons W.B., Hines M.E. and Macumber P.G. (1992) – *Formation of alunite, jarosite and hydrous iron oxides in a hypersaline system lake Tyrrell, Victoria, Australia.* Chem. Geol., **96**,183-202.

Mesaed A.A. and Surour A.A. (1999) – *Mineralogy and geochemistry of the Bartonian stratabound diagenetic and lateritic glauconitic ironstones of El-Gideda mine, Bahria Oasis, Egypt.* International Conference on the Geology of the Arab World, Cairo Univ., Egypt, 509-540.

Muller J. P and Bocquier G. (1985) – *Textural and mineralogical relationships between ferruginous nodules and surrounding clayey materials in a laterial from Cameroon.* Proceedings of the Intern. Clay Conf., Denver, 186-194.

Mutlu H., Sariiz K. and Kadir S. (2005) – *Geochemistry and origin of the Şaphane alunite*

deposit, Western Anatolia Turkey. Ore Geol. Rev., **26**, 39-50.

NAGASAWA K. (1978) – *Kaolinite minerals*. Development in Sedimentology, **26**, 189-219.

POLYAK V.J. and GÜVEN N. (1996) – *Alunite, natroalunite and hydrated halloysite in Carlsbad Cavern and Lechuguilla Cave, New Mexico.* Clays Clay Min., **44**, 843-850.

POLYAK V.J. and PROVENCIO P. (1998) – *Hydrobasaluminuite and aluminite in Caves of the Guadalupe mountains, New Mexico.* J. Cave Karst studies, **60**, 51-57.

POLYAK V.J. and GÜVEN N. (2000) – *Clays in the cave of the Guadalupe Mountains, New Mexico,* J. Cave Karst studies, **62**, 120-126.

POLYAK V.J. and PROVENCIO P. (2001) – *Byproduct materials related to H_2S-H_2SO_4 influenced speleogenesis of Carlsbad, Lechuguilla, and other Caves of the Guadalupe mountains, New Mexico* J. Cave Karst studies **63**, 23-32.

RUSSELL J.D. and FRASER A.A. (1995) – *Infrared methods*. In: Clay Mineralogy (M.J. Wilson, editor). Chapman and Hall, London, 11-69.

RYE R.O., BETHKE P.M. and WASSERMAN M.D. (1992) – *The stable isotope geochemistry of acid sulfate alteration,* Econ. Geol. **87**, 225-262.

SAID R. (1990) – *The geology of Egypt,* Elsevier, New York 734 pp.